n- and Isoalkane Adsorption Mechanisms on Zeolite MCM-22

Joeri F. M. Denayer,*,† Refik A. Ocakoglu,† Joris Thybaut,‡ Guy Marin,‡ Pierre Jacobs,§ Johan Martens,§ and G. V. Baron†

Dienst Chemische Ingenieurstechniek, Vrije Universiteit Brussel, Pleinlaan 2, B-1050 Brussel, Belgium, Laboratorium voor Petrochemische Techniek, Universiteit Gent, Krijgslaan 281, B-9000 Gent, Belgium, and Centrum voor Oppervlaktechemie en Katalyse, Katholieke Universiteit Leuven, Kasteelpark Arenberg 23, B-3001 Leuven, Belgium

Received: January 31, 2006; In Final Form: March 16, 2006

Low-coverage adsorption properties (Henry constants, adsorption enthalpy, and entropy) of linear and branched alkanes (C3−C8) on zeolite MCM-22 were determined using the chromatographic technique at temperatures between 420 and 540 K. It was found that adsorption enthalpy and entropy of linear alkanes vary in a nonmonotonic way with carbon number. The adsorption behavior of alkanes was rationalized on the basis of the pore geometry. Short molecules prefer to reside in the pockets of the MCM-22 supercage, where they maximize energetic interaction with the zeolite. Longer molecules reside in the larger central part of the supercage. For carbon numbers up to six, singly branched alkanes are selectively adsorbed over their linear counterparts. This preference originates from the entropic advantage of singly branched molecules inside MCM-22 supercages, where these species have high rotational freedom because of their small length.

Introduction

Pore diameters of zeolites measure typically 5−10 Å and are comparable to the dimensions of many industrially important molecules, such as alkanes, having diameters of 4−6 Å. This close matching gives rise to substantially different adsorption states for even physicochemically related molecules in a given zeolite pore. On the basis of this shape-selective feature, highly effective molecular separations and selective catalytic conversions can be achieved within zeolitic structures that are difficult to accomplish with other materials and/or techniques.[1−3]

So far, several shape-selectivity mechanisms have been elucidated and applications identified.[2−18] In common molecular sieving, bulky molecules adsorb preferentially over bulkier species as a result of steric constraints imposed by the zeolites' framework, e.g., linear alkane molecules compared to branched isomers.[19−23] Besides this common adsorption competition based on molecular bulkiness, the reverse phenomenon can also occur, i.e., competitive adsorption in favor of the bulkier species. Experiments revealed preferential adsorption of branched alkanes over their linear isomers on specific zeolites with tubular pore systems such as SAPO-5 and Mordenite.[24−28] Molecular simulations indicated that in such zeolites, depending on conditions, branched alkanes are preferentially adsorbed at the expense of linear isomers.[29−34]

The present manuscript discusses the mechanisms of shape selectivity in *n*- and isoalkane adsorption on zeolite MCM-22. This zeolite with IZA code MWW is a relatively new synthetic material that has an unusual and quite complex pore structure.[35] Its framework is composed of two independent pore systems. One of these systems is defined by two-dimensional sinusoidal channels, which maintain an effective 10-ring diameter (0.40 × 0.55 nm^2) throughout the structure. The intersections of these channels result in small cages with dimensions of 0.64 × 0.69 nm^2.[36] The other pore system is composed of large supercages whose inner free diameter of 0.71 nm is defined by 12-MR and whose inner height is 1.82 nm. Figure 1 sketches the framework connectivity in the wall of one supercage of MCM-22 zeolite. Access to these cages is through six 10-rings, which have dimensions of 0.42 × 0.51 nm^2. The 10- and 12-MR combination produces a large ellipsoidal void space in the center of the supercage with a diameter of 1.64 nm and a height of 0.42 nm. The supercage is symmetric in the plane that is normal to the page; i.e., the diameter of the pockets normal to the page is 0.71 nm. For the ellipsoid, the diameter of 1.64 nm is conserved in all directions. As a result of this architecture, the supercage can be divided into three imaginary segments: two identical pockets at the top and the bottom and one large section in the middle (Figure 1). In addition to the internal pore systems, the external surface of MCM-22 contains cups. These cups, referred to as surface pockets or chalices in the literature, are identical to the top and bottom pockets of the supercage. This pore

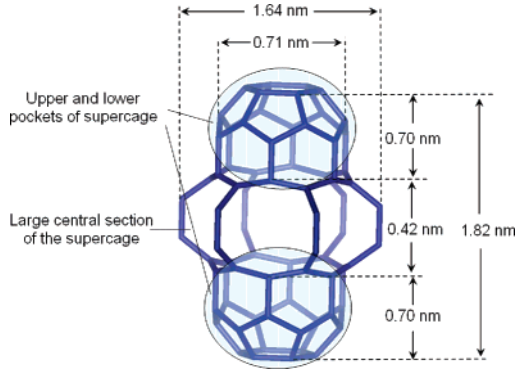

Figure 1. Illustration of the supercage of MCM-22. Access to the supercage is through the 10-rings in the central section. Indicated distances correspond to the free volume inside the supercage.

* To whom correspondence should be addressed. E-mail: Joeri.Denayer@vub.ac.be, Tel: +32 2 629 17 98, Fax: +32 2 629 32 48.
† Vrije Universiteit Brussel.
‡ Universiteit Gent.
§ Katholieke Universiteit Leuven.

10.1021/jp060657s CCC: $33.50
Published on Web 04/13/2006

TABLE 1: Adsorbent and Column Properties

zeolite properties	
Si/Al	30
N2 micropore volume (mL/g)	0.187
BET surface area (m^2/g)	460.4
t-plot surface area (m^2/g)	34.9
column properties	
length (m)	0.35
inner diameter (mm)	2.16
packed adsorbent mass (g)	0.446
carrier (He) flowrate (mL/min)	20

structure of MCM-22 intrigued many researchers in the past decade. A large number of publications on issues such as characterization of the pore structure, the role of the different pore systems in catalytic reactions, and adsorption and diffusion characteristics of zeolite MCM-22 appeared during this period.[37−52]

Here, low-coverage adsorption of linear and branched alkanes (C3−C8 range) was examined using the pulse chromatographic technique. Henry constants, limiting adsorption enthalpies, and entropies were determined. An attempt is made to explain the remarkable shape-selective adsorption properties of MCM-22 on the basis of the peculiar micropore structure of this zeolite.

Experimental Methods

Zeolite Na-MCM-22 was synthesized according to the recipe of Bundens et al.[6] Characteristics of the synthesized Na-MCM-22 sample are given in Table 1. The zeolite powders were compacted into disks by applying a pressure of ca. 30 MPa. The disks were then broken into fragments and sieved. The 400−500 μm fraction was filled into a 1/8 in. diameter stainless steel column with a length of 0.35 m (see Table 1 for further column properties). This column was placed in a HP-4890 gas chromatograph (GC) equipped with a thermal conductivity detector (TCD). In situ activation of the adsorbent was performed by raising the temperature from ambient to 383 K at a rate of 1 K/min and maintaining the temperature for 30 min, then from 383 to 523 K by 2 K/min, maintaining the temperature for 2 h, and finally from 523 to 723 K, maintaining the temperature for 6 h. Helium was used as the carrier gas.

The pulse chromatographic technique was used to determine the adsorption equilibrium.[3] Henry adsorption constants were determined from the first moment of the response curve on the TCD after injection of an alkane trace. Adsorption enthalpy and entropy were obtained by fitting the temperature dependence of the Henry constant to the van't Hoff equation. A detailed description of the calculation method can be found elsewhere.[53]

Results

Figure 2 depicts chromatograms obtained at 493 K on MCM-22 when different volumes of alkane were injected. The injection volume had no effect on the responses of linear and singly branched alkanes (Figure 1a,b), meaning that adsorption occurred in the linear part of the isotherm-termed Henry region. For the linear and singly branched alkanes, injection volumes of 0.001 μL liquid were used through the whole set of experiments. In contrast, the retention time of multi-branched isomers increased with decreasing amount of injection, and the shape of the response curves was clearly non-Gaussian, except for the lowest amount injected (only 2,2,4-trimethylpentane shown in Figure 1c). Experiments with multi-branched isomers were conducted using 0.001 μL sample volumes taken from the vapor phase in equilibrium with the liquid at room temperature. The detection limit of the experimental setup did not allow injecting amounts lower than 0.001 μL of vapor. Henry constants were calculated from the first moment of the chromatographic response curve obtained with this injection volume. It should be emphasized that with this minute amount of injection, the criterion for adsorption in Henry regime might not be met. However, the van't Hoff plots of multi-branched species were highly linear and the response curve was Gaussian for this concentration. This indicates that the experiments were performed in the very vicinity of the linear part of the adsorption isotherm. Nonetheless, the values reported for multi-branched isomers should be considered as lower bounds of Henry constants.

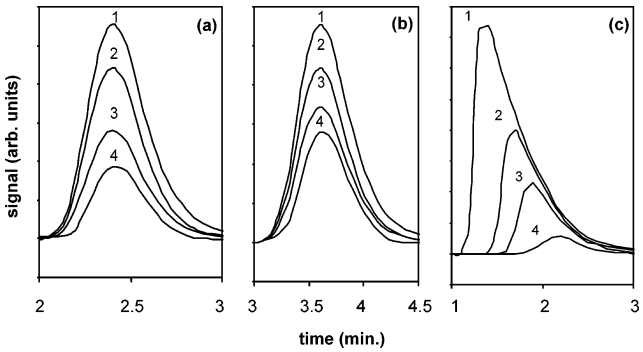

Figure 2. Effect of amount of injection on the chromatographic responses. (a) *n*-C6, (b) 3-MeC5, and (c) 2,2,4-TriMeC5. All chromatograms are measured at 493 K. Numbers 1, 2, 3, and 4 represent injections of 0.01 μL liquid, 0.005 μL liquid, 0.001 μL liquid, and 0.001 μL vapor, respectively.

Henry Constants. Chromatographic responses of mixtures of linear and branched alkanes (*n*-C4 and iso-C4; *n*-C5 and 2-MeC4; *n*-C6, 3-MeC5, and 2,2-DiMeC4) on Na-MCM-22 at 473 K are shown in Figure 3. In each case, the singly branched isomer is retained longer than its linear skeletal alkane. The families of iso- and *n*-alkanes were entirely separated. This is in contrast to what is observed with most other zeolites, where the linear molecule is preferentially adsorbed over its singly branched isomer.[19−23] Among the investigated molecules, in some instances, there is conformity with conventional shape selectivity. The monobranched isomer 2-MeC6 adsorbs less strongly than heptane (not shown). The doubly branched isomer adsorbed the weakest among the hexane isomers (2,2-dimethylbutane in Figure 3c).

Figure 4 depicts the Henry constants (K') of linear and branched alkanes on Na-MCM-22 at 493 K. All the other measured K' values are reported in Table 2, together with data from literature.[54] Although experimental conditions and techniques were quite different (pulse chromatography at 423−543 K versus gravimetry calorimetry at 323 K), there is a good match between the K' values reported in the present work (extrapolated to 323 K using the van't Hoff relation) and the values of Eder et al. Yet, it should be emphasized that these authors have calculated (by extrapolating the adsorption isotherm to the zero-coverage limit) higher Henry constants for the linear pentane compared to its isomer, 2-MeC4.

Henry constants of linear alkanes show an exponential dependency on carbon number, but this relationship is less regular on Na-MCM-22, as commonly observed for zeolites (Figure 4).[55,56] The studied carbon-number range of singly branched alkanes is too short to comment on the trend of K' values. However, it should be noted that the K' value of 2-MeC5 lies almost on the same level as 2-MeC4, contradicting to the typical increase of Henry constants with carbon number (Table 2).[55,56] Further, 3-MeC5 has a noticeably higher Henry constant

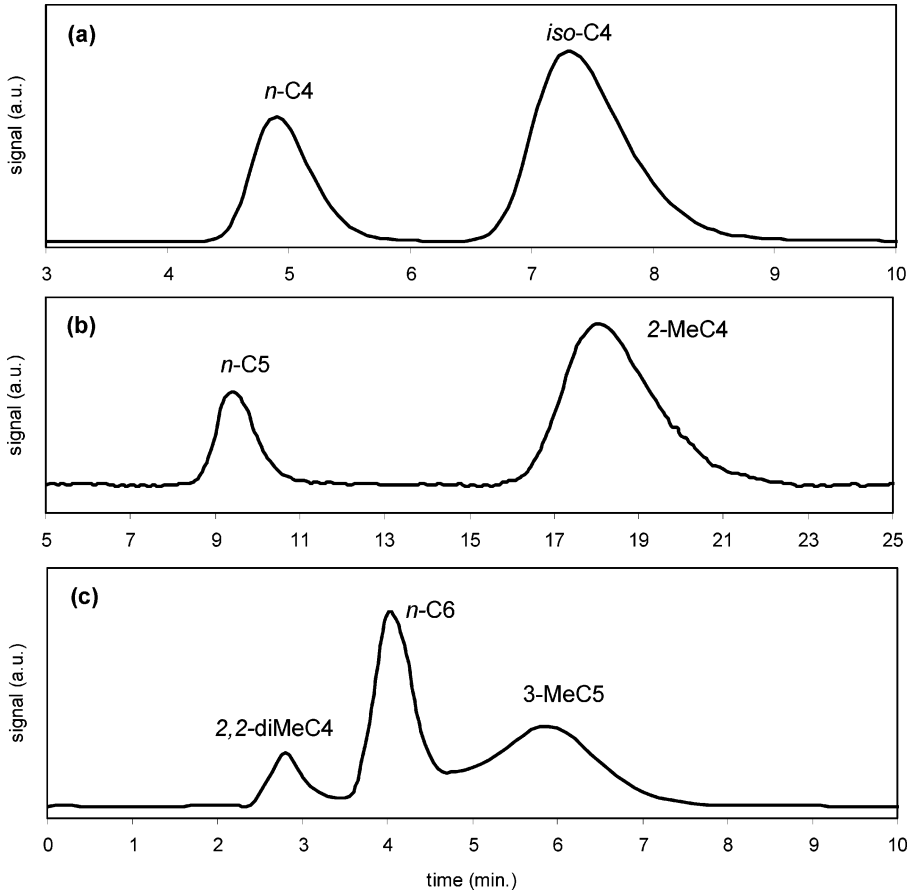

Figure 3. Chromatograms of hydrocarbon mixtures showing inverse shape selectivity on zeolite MCM-22 (473 K). (a) Mixture of *n*-C4 and *iso*-C4, (b) mixture of *n*-C5 and 2-MeC4, (c) mixture of *n*-C6, 3-MeC5, and 2,2-DiMeC4.

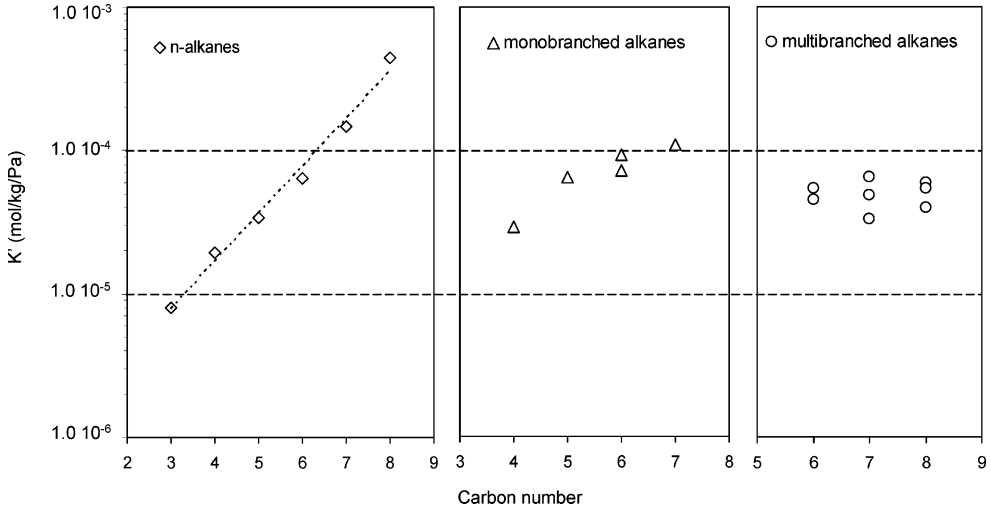

Figure 4. Henry constants (K′) of *n*- and *iso*-alkanes at 493 K on MCM-22.

than 2-MeC5, which is unusual on zeolites operating according to classical shape-selectivity schemes, where generally adsorption is in favor of the 2-methyl branched isomer.[21−23] However, preferential adsorption of 3-MeC5 over 2-MeC5 was already observed at higher degrees of pore filling on zeolite ZSM-5, where the more symmetrical 3-MeC5 packs more efficiently in the intersecting pore system of this zeolite.[19,57]

Henry constants of iso-C4, 2-MeC4, 2-MeC5, and 3-MeC5 are higher than those of their linear isomers. The reverse holds for 2-MeC6 and *n*-C7. Henry constants of multi-branched alkanes are noticeably lower than their corresponding linear isomers, and the differences increase with increasing chain length. Although there is a difference of 3 carbon atoms between the smallest and the largest multibranched alkane (e.g., 2,2-dimethylbutane and 2,2,4-trimethylpentane), the Henry constants do not differ significantly from each other and no simple relationship with the chain length can be drawn from the present results. Furthermore, there was no notable effect of branching location along the main carbon chain.

Adsorption Enthalpies. Adsorption enthalpies, as derived from the slopes of the van't Hoff plots, are depicted in Figure 5 and tabulated in Table 3, together with values found in the literature. Generally, the adsorption enthalpies increase with carbon number for linear alkanes, yet not in a strictly linear

TABLE 2: Measured Henry Constants (in mol/kg/Pa) on Zeolite Na-MCM-22 at Different Temperatures

T (K)	323[a]	323[b]	423	433	443	458	473	483	493	503	513	523	533	543
n-C3	2.0 10^{-3}	1.6 10^{-3}	4.2 10^{-5}	3.3 10^{-5}	2.4 10^{-5}	1.8 10^{-5}	1.2 10^{-5}	9.8 10^{-6}	8.1 10^{-6}	6.7 10^{-6}				
n-C4	1.4 10^{-2}	1.0 10^{-2}	1.4 10^{-4}	1.0 10^{-4}	7.2 10^{-5}	4.9 10^{-5}	3.2 10^{-5}	2.5 10^{-5}	2.0 10^{-5}	1.5 10^{-5}				
n-C5	6.4 10^{-2}	3.8 10^{-2}	3.1 10^{-4}		1.5 10^{-4}	9.6 10^{-5}	5.9 10^{-5}	4.4 10^{-5}	3.4 10^{-5}	2.6 10^{-5}	2.1 10^{-5}	1.6 10^{-5}		
n-C6	4.2 10^{-1}	1.9 10^{-1}			3.6 10^{-4}	2.1 10^{-4}	1.2 10^{-4}	8.6 10^{-5}	6.4 10^{-5}	4.8 10^{-5}	3.6 10^{-5}	2.8 10^{-5}		
n-C7							2.9 10^{-4}	2.0 10^{-4}	1.5 10^{-4}	1.1 10^{-4}	7.7 10^{-5}	5.8 10^{-5}	4.4 10^{-5}	3.3 10^{-5}
n-C8									4.4 10^{-4}	3.0 10^{-4}	2.2 10^{-4}	1.5 10^{-4}	1.1 10^{-4}	8.4 10^{-5}
2-MeC3			2.2 10^{-4}	1.6 10^{-4}	1.1 10^{-4}	7.3 10^{-5}	4.8 10^{-5}	3.7 10^{-5}	2.9 10^{-5}	2.3 10^{-5}				
2-MeC4					2.9 10^{-4}	1.8 10^{-4}	1.1 10^{-4}	8.4 10^{-5}	6.4 10^{-5}	4.9 10^{-5}	4.0 10^{-5}	3.0 10^{-5}		
2-MeC5	1.2 10^{-1}	1.4 10^{-1}			3.8 10^{-4}	2.2 10^{-4}	1.3 10^{-4}	9.7 10^{-5}	7.3 10^{-5}	5.5 10^{-5}	4.2 10^{-5}	3.3 10^{-5}		
3-MeC5					4.8 10^{-4}	2.8 10^{-4}	1.7 10^{-4}	1.3 10^{-4}	9.4 10^{-5}	7.0 10^{-5}	5.4 10^{-5}	4.1 10^{-5}		
2-MeC6							2.1 10^{-4}	1.3 10^{-4}	1.1 10^{-4}	7.5 10^{-5}	5.3 10^{-5}	4.2 10^{-5}	3.2 10^{-5}	2.5 10^{-5}
2,2-DMeC4					2.5 10^{-4}	1.5 10^{-4}	8.8 10^{-5}	6.3 10^{-5}	4.5 10^{-5}	3.4 10^{-5}	2.5 10^{-5}	1.9 10^{-5}		
2,3-DMeC4					3.1 10^{-4}	1.8 10^{-4}	1.0 10^{-4}	7.5 10^{-5}	5.4 10^{-5}	4.0 10^{-5}	3.0 10^{-5}	2.3 10^{-5}		
2,2,4-TMeC5					3.8 10^{-4}	2.0 10^{-4}	1.1 10^{-4}	7.8 10^{-5}	5.4 10^{-5}	3.9 10^{-5}	2.8 10^{-5}	2.0 10^{-5}		

[a] Eder et al., (1996).[54] [b] This study, extrapolated using the van't Hoff relation.

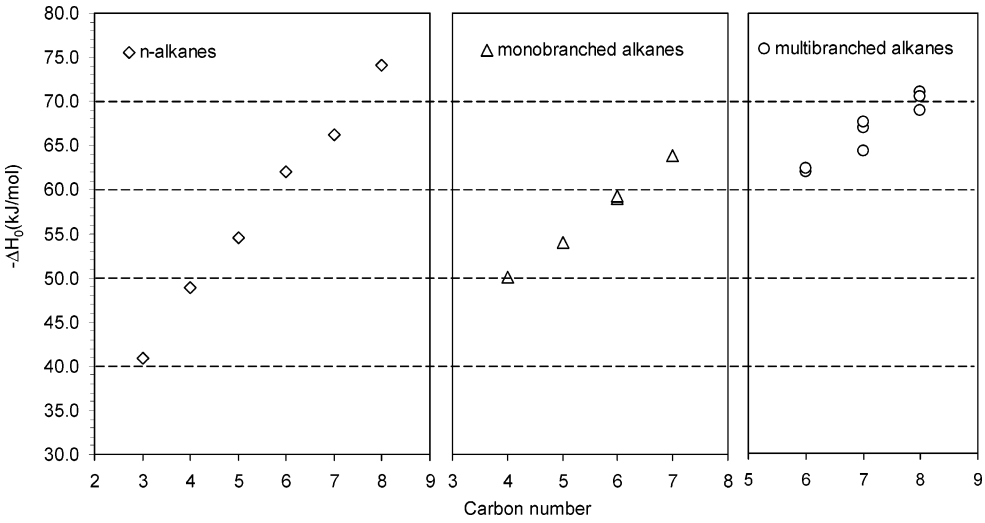

Figure 5. Adsorption enthalpies on Na-MCM-22.

way as is generally observed for homologues series of alkanes.[55−57] For instance, between propane and butane, there is 8 kJ/mol difference, whereas it is only 4 kJ/mol between *n*-hexane and *n*-heptane, again increasing to 8 kJ/mol when going from *n*-heptane to *n*-octane. Although the present values are systematically lower than those obtained using calorimetry (Table 3), the differences between pairs of linear alkane molecules are similar. Eder et al. also found that the largest increment in enthalpies is between propane and *n*-butane. For the singly branched molecules, the small range of carbon atoms that was examined does not allow setting a precise conclusion in terms of carbon-number dependency. The adsorption enthalpy of 2-MeC4 is 4 kJ/mol higher than 2-MeC3 (isobutane), and the former molecule has a 5 kJ/mol lower enthalpy than 2-MeC5. The adsorption enthalpies of 2- and 3-MeC5 are similar. Except in the case of isobutane, the enthalpies of singly branched species are slightly lower than those of the linear isomers. For isobutane, the measured enthalpy exhibits a very high value (50.1 kJ/mol), which is even higher than that for *n*-butane. Finally, for the multi-branched alkanes, there is about 4.0 kJ/mol increase in adsorption enthalpy per additional carbon. Remarkably, position nor number of branches matters. In absolute values, the adsorption enthalpies of multi-branched alkanes are close to those of their corresponding linear and singly branched isomers, despite their lower Henry constant.

Figure 6 depicts the adsorption enthalpy per carbon atom of a given linear alkane on several zeolites.[23,55] These values were obtained by dividing the adsorption enthalpy of a molecule by its carbon number. The enthalpy per carbon atom decreases with increasing chain length on zeolite Na-MCM-22 in contrast to common zeolites, where values are almost chain-length independent. The enthalpy contribution per carbon atom is 13.6 kJ/mol/-CH_x for propane compared to 9.3 kJ/mol/-CH_x for *n*-octane on Na-MCM-22. In Na-MCM-22 the adsorbate−adsorbent

TABLE 3: Adsorption Enthalpies and Preexponential Factors on Na-MCM-22

	$-\Delta H_0$ (in kJ/mol)			K'_0
	this study	Eder et al., 1996[54]	Du et al., 2000[70]	(in mol/kg/Pa)
n-C3	40.9 ± 0.3	49		$(3.8 \pm 0.1)\ 10^{-10}$
n-C4	48.8 ± 0.4	59		$(1.3 \pm 0.1)\ 10^{-10}$
n-C5	54.5 ± 0.3	64		$(5.8 \pm 0.1)\ 10^{-11}$
n-C6	62.0 ± 0.6	69	38.1	$(1.8 \pm 0.2)\ 10^{-11}$
n-C7	66.3 ± 0.3			$(1.4 \pm 0.1)\ 10^{-11}$
n-C8	74.2 ± 0.6			$(6.1 \pm 0.2)\ 10^{-12}$
2-MeC3	50.1 ± 0.3			$(1.4 \pm 0.1)\ 10^{-10}$
2-MeC4	54.1 ± 0.3			$(1.2 \pm 0.1)\ 10^{-10}$
2-MeC5	59.0 ± 0.4	64		$(4.2 \pm 0.1)\ 10^{-11}$
3-MeC5	59.3 ± 0.2		36.4	$(4.9 \pm 0.1)\ 10^{-11}$
2-MeC6	63.9 ± 0.2			$(1.7 \pm 0.2)\ 10^{-11}$
2,2-DMeC4	62.0 ± 0.3			$(1.2 \pm 0.1)\ 10^{-11}$
2,3-DMeC4	62.4 ± 0.1			$(1.3 \pm 0.1)\ 10^{-11}$
2,2,4-TMeC5	70.5 ± 0.4			$(1.8 \pm 0.2)\ 10^{-12}$

matching within the *n*-alkane homologous family does not follow the regular pattern.

Preexponential Factors (Adsorption Entropy). The preexponential factors K'_0, are plotted against carbon number in Figure 7 and listed in Table 3. The logarithm of the preexponential factor is directly related to the adsorption entropy at zero coverage considering that $\ln K'_0 = \Delta S_0 + \text{constant}$.[24,60,61] A higher preexponential factor corresponds to a lower loss of entropy change upon adsorption. In analogy to the adsorption enthalpies on Na-MCM-22, there is no evident trend in the preexponential factors of *n*-alkanes. K'_0 appears to decrease exponentially from propane to hexane. In this *n*-alkane series, there is a linear variation of adsorption entropy with carbon number. Heptane and octane deviate from this trend. Furthermore, preexponential factors of singly branched molecules do not display a clear tendency with carbon number. K_0' of 2-MeC3 is very close to 2-MeC4, but the values for 2-MeC5 and 3-MeC5 are noticeably lower. The absence of an apparent trend in the preexponential factors of isoalkanes with carbon number again indicates that the confinement of individual adsorbates (linear and singly branched) inside Na-MCM-22 pores is different in each case. Preexponential factors of multibranched alkanes with side branches at the same position decrease exponentially with increasing chain length (see 2,2-DMeC4, 2,2-DMeC5, and 2,2-DMec6 in Table 3). For the other multibranched molecules, the limited number of molecules studied does not allow commenting explicitly on carbon-number dependency.

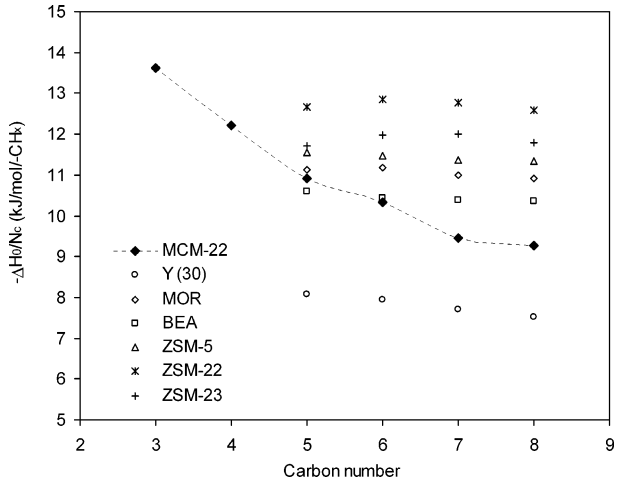

Figure 6. Adsorption enthalpies per carbon atom on different zeolites[23,55] (the dashed line is merely a guide to the eye).

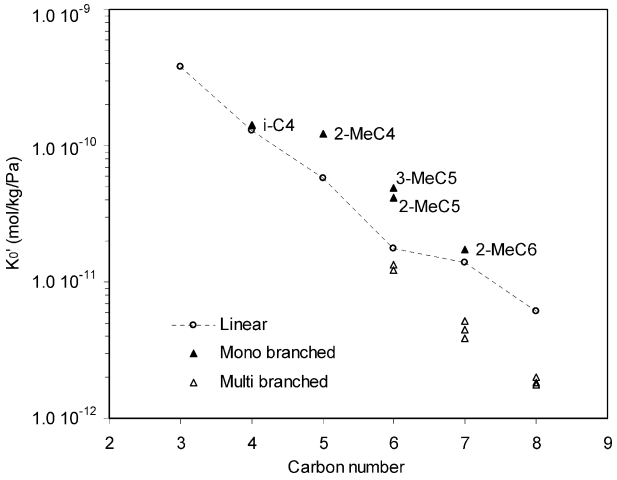

Figure 7. Preexponential factors on Na-MCM-22 (the dashed line is merely a guide to the eye).

Discussion

Zeolite Na-MCM-22 shows peculiar adsorption selectivity, in that it prefers adsorbing monobranched C4−C6 alkanes over their linear isomers, whereas multibranched alkanes are adsorbed to the lowest extent. That the monobranched alkanes are preferentially adsorbed compared to their linear isomers means that their Gibbs' free energy of adsorption is more negative. Monobranched alkanes have a combination of adsorption enthalpy and entropy that renders their adsorption favorable compared to linear chains. For isobutane, the adsorption enthalpy is slightly larger than for butane. For the other monobranched alkanes (2-MeC4, 2-MeC5, and 3-MeC5), the adsorption enthalpy is lower than for their linear isomer (Table 3). The selective adsorption of the monobranched alkanes can, thus, not be attributed to enthalpy differences. Monobranched alkanes have higher preexponential factors than linear alkanes (Table 3). This means that the monobranched alkanes have a less negative adsorption entropy and, thus, lose less freedom in the transition from the bulk gas state to the adsorbed state. Hence, the selective adsorption of monobranched alkanes is driven by entropic rather than energetic effects.

The above detailed interplay between the adsorption enthalpy and entropy can be visualized via a compensation chart, where these two thermodynamic properties are plotted against each other. On regular zeolite materials, these charts display in linear trends for a given hydrocarbon family.[54,58,62−66] Figure 8 depicts the compensation chart for linear and branched alkanes on MCM-22. From C3 to *n*-C6, the logarithm of the preexponential factor increases linearly with the adsorption enthalpy. A discontinuity is seen between *n*-C6 and *n*-C7, pointing at a different adsorption mode from *n*-C7 on. On a relative basis, *n*-C7 and *n*-C8 lose less freedom for a certain interaction energy compared to the shorter *n*-alkanes. Furthermore, the chart of Figure 8 shows that the monobranched isomers have an entropic advantage over the linear ones, manifesting the inverse shape selectivity. The multibranched alkanes lie above the linear alkanes in the compensation chart, meaning that these molecules have no entropic advantage.

This analysis of enthalpy and entropy constitutes the basis of our approach to identify the adsorption sites for the different alkanes. MCM-22 has two independent pore systems, each offering several potential adsorption sites. The 10-MR system is constituted by slender sinusoidal channels, but these channels cross each other, creating somewhat larger intersections. Besides, MCM-22 contains large supercages with short bridges that

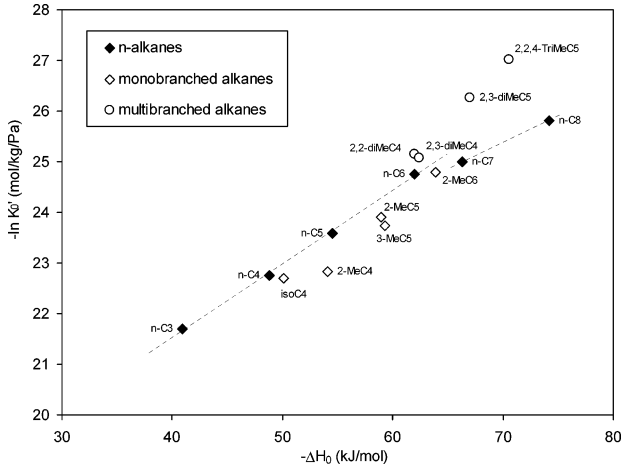

Figure 8. Compensation chart for adsorption of linear, monobranched, and multibranched alkanes on Na-MCM-22.

TABLE 4: Comparison of Radius of Gyration R_g with the Radius of the Supercage

	L^a (Å)	R_g (Å)	$R_g/R_{c1}{}^b$	$R_g/R_{c2}{}^c$
C4	7.6	7.67	0.97	0.80
C5	8.8	8.88	1.12	0.93
C6	10.1	10.37	1.31	1.08
C7	11.4	11.66	1.47	1.21
iC4	6.3	6.78	0.85	0.71
2MeC4	7.6	7.87	0.99	0.82
2MeC5	8.8	9.45	1.19	0.98
3MeC5	8.8	9.13	1.15	0.95
2MeC6	10.1	10.31	1.30	1.07

[a] Length of the molecule. [b] Radius in the central section of the supercage. [c] Radius in the upper and lower pockets of the supercage.

interconnect these cages. Molecular dynamics simulations showed that diffusion of 2-MeC6 in MCM-22 (between 450 and 850 K) in the sinusoidal 10-MR channels does not occur to a significant extent.[67] That study also stated that intercage diffusion (in the short bridges that connect the neighboring supercages) does not happen (for *n*-C7 and 2-MeC6) until elevated temperatures so that molecules spend most of their time inside the cage. In an NMR study of xenon adsorption in zeolite MCM-22, it was found that, particularly at low coverage, xenon atoms predominantly prefer to locate inside the supercages.[68] During the discussions of infrared spectrometric (IR) results,[69] it was declared that the supercages constitute about 70% of the micropore volume, indicating that the majority of the adsorption phenomenon is happening there. This argument was strengthened by the modeling calculations.[70] The authors determined the adsorption isotherm of *n*-C6 and 3-MeC5 at various temperatures on ITQ-1, the pure silica analogue of MCM-22, and suggested that three out of four adsorbate molecules are located in the large cages and one molecule in the sinusoidal channel system, which is in agreement with the supremacy of adsorption inside the supercages. In summary, on the basis of supporting information from literature, adsorption of linear and singly branched molecules will be considered, occurring principally inside the supercages of MCM-22.

As the adsorbed molecules, whether they are linear or branched, are confined in a closed space, i.e., the supercage, their losses in translational and vibrational degrees of freedom will be comparable. Differences in rotational freedom in the supercages of MCM-22 may have a substantial impact on the adsorption equilibrium. Rotational entropy of the different species was qualitatively analyzed by comparing the radius of gyration of each molecule to the available space in the

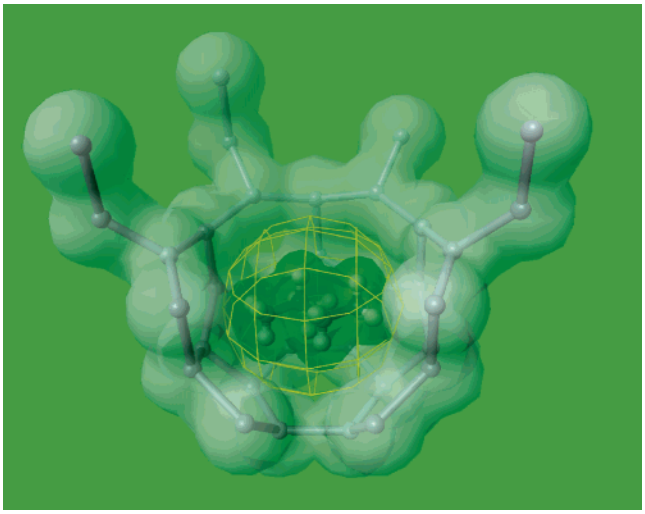

Figure 9. Drawing of 2-methylbutane in the lower pocket of the MCM-22 supercage. Yellow sphere represents the Gyration sphere circumscribing the rotational movement of the molecule around its center of gravity. The van der Waals contact surface of zeolite and adsorbed molecule are represented by a transparent surface.

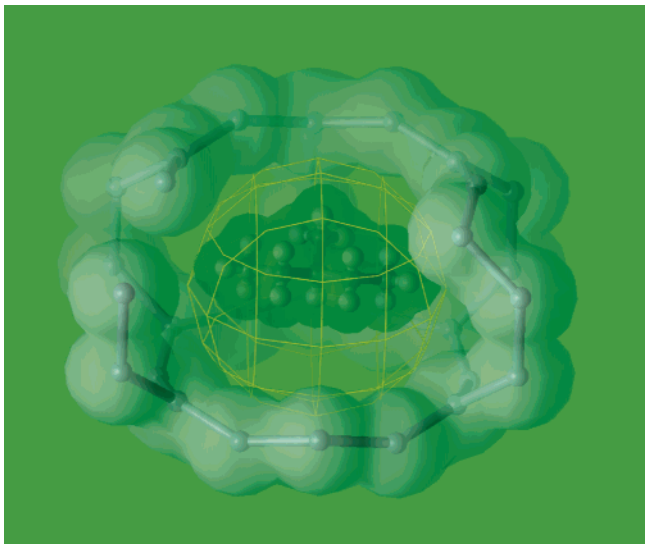

Figure 10. 2-methylpentane molecule in the central part of the MCM-22 supercage.

supercage. Molecular diameters and lengths were calculated assuming that these properties can be best represented by van der Waals volumes of the molecule. From these dimensions, the radius of gyration R_g was calculated, assuming rotation around the center of mass. This radius was then compared to the radius of the largest sphere that fits into the van der Waals contour of the cage (R_c), differentiating between two adsorption spots inside the supercage. These are the upper and lower pockets and the large central section of the supercage (see Figure 1). In Table 4, the R_g values of each adsorbate is compared to R_c of the pockets ($R_{c,p}$) and the central section ($R_{c,c}$) separately. This comparison provides an estimate of the ability of a molecule to rotate in different sections of a supercage of MCM-22. A ratio higher than unity denotes that this particular molecule is larger than the pockets or the central section, consequently designating if it can rotate freely therein or not.

For pentane and 2-MeC4, the gyration sphere of the branched isomer neatly fits in the pockets of the supercage, whereas rotation of *n*-C5 in there is already severely restricted (Figure 9). Both components retain their rotational freedom in the larger central section. A linear hexane molecule is able to rotate neither

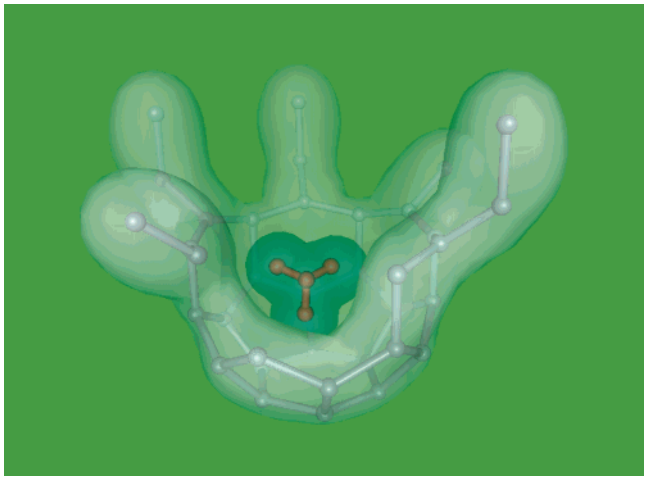

Figure 11. Drawing of *iso*-butane adsorption in the pocket of the MCM-22 supercage.

inside the pockets nor inside the central section, whereas the shorter 2-MeC5 and 3-MeC5 are still able to rotate inside the central section (Figure 10), resulting in a lower loss of entropy (Figure 8). Butane and isobutane are both able to rotate freely inside the pockets and the central section of the supercage, which is in agreement with the low difference in adsorption entropy between both molecules, as shown in Figure 8. However, the adsorption enthalpy of isobutane is unusually high and also is higher than that of butane (Table 3). The spherical shape of this former isomer closely fits into the pockets of the supercage, where it not only interacts with framework atoms of the side walls but also with those of the bottom of the pocket (see Figure 11). In this way, a higher energetic interaction is obtained compared to that of butane. From a carbon number of 7 on, the monobranched alkanes become too large to rotate in the MCM-22 supercages. In this case, both molecules have R_g/R_c values greater than unity for both the pockets and the central section, which means that the advantage of shorter length in terms of rotational entropy is lost. Indeed, heptane adsorbs preferentially over its branched isomer 2-MeC6 in contrast to the above-mentioned alkane couples (Table 2).

The above considerations concerning supercage adsorption shed a light on the unusual decrease of adsorption enthalpy per carbon atom with increasing chain length (Figure 6). Short linear alkanes (from methane to butane) can reside as a whole inside the pockets where all of their end hydrogen atoms can interact closely with the pore walls, as shown in Figure 12. This results in large interaction energies (adsorption enthalpies) for these molecules and a large increment in adsorption enthalpy per additional carbon atom. But when the chain length increases, the molecule grows toward the central section of the supercage, where there is a much larger free space. As a result of this cage enlargement, the additional carbon atoms will interact to a lesser extent than the atoms residing in the depths of the pocket, explaining the aforementioned enthalpy effect. Whereas butane is at the limit, pentane is too long to reside completely in the pocket and has at least one methyl group in the central section, where the distance between the hydrogen atoms and the atoms of the framework is larger, explaining the lower difference in adsorption enthalpy between *n*-C4 and *n*-C5 (5.7 kJ/mol) compared to that of *n*-C4 and *n*-C3 (7.9 kJ/mol). The same reasoning is valid for *n*-C6. To explain the discontinuity between *n*-C6 and *n*-C7 in the compensation chart (Figure 8), a different adsorption configuration is proposed, in which the molecules remain as a whole in the central section of the supercage (see Figure 12), where the entropy loss is expected to be lower than in the pockets of the cage.

The low adsorption of multibranched species, the absence of any significant shape selectivity, the invariance of Henry constants on branching position, and dependency of retention time on injection volume for multibranched alkanes can be readily explained by their large kinetic diameter (>0.6 nm) compared to the size of the 10-membered rings (10-MR) giving access to both the supercages (0.42×0.51 nm^2) and two-dimensional sinusoidal channels (0.40×0.55 nm^2), preventing their intra-pore adsorption. Despite this, the multibranched alkanes have adsorption enthalpies very close to those of the linear chains (e.g., *n*-octane: 74.2 kJ/mol and isooctane: 70.5 kJ/mol), which is not expected for nonselective adsorption on the crystal outer surfaces. This large energetic interaction could be the result of adsorption in the cups on the external surface of the MCM-22 crystals, for which it was shown that they can participate in the adsorption/reaction of guest molecules.[43, 71]

Conclusions

Pulse chromatographic experiments revealed peculiar alkane adsorption mechanisms in zeolite Na-MCM-22. The large supercages of this material accommodate linear and monobranched alkanes, whereas multibranched alkanes are excluded as they are not capable to diffuse through the 10-MR windows connecting the supercages. The small apertures of these 10-MR windows also restrict the translational motion of linear and monobranched alkanes between adjacent cages, such that rotational motion of the molecules becomes a critical factor with respect to the adsorption entropy. Monobranched alkanes, with

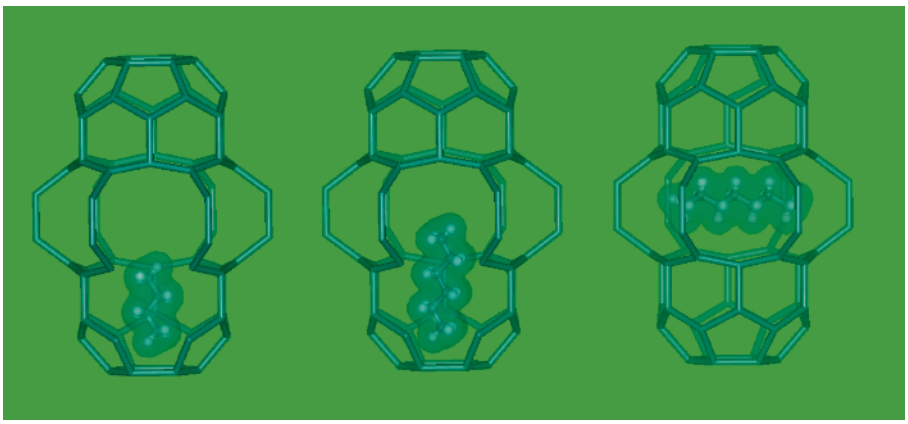

Figure 12. Adsorption of linear alkanes inside a MCM-22 supercage. (Left) *n*-Butane in pocket. (Middle) *n*-Hexane in pocket and central section. (Right) *n*-Heptane in central section.

their shorter chain length, have a smaller radius of gyration compared to the linear alkanes. As a result, monobranched alkanes still can rotate inside the pockets or central part of the supercage, whereas the linear chains are severely restricted in their rotational motion. Consequently, monobranched alkanes retain more rotational freedom, which offers them an entropic advantage, leading to their preferential adsorption in comparison to the linear chains.

Acknowledgment. J.D. is grateful to the F.W.O.-Vlaanderen, for a fellowship as postdoctoral researcher. The involved teams are participating in the IAP-PAI programme (IUAP IV-11) on Supramolecular Chemistry and Catalysis, sponsored by the Belgian Federal Government.

References and Notes

(1) Van Bekkum, H.; Flanigen, E. M.; Jacobs, P. A.; Jansen, J. C. *Introduction to Zeolite Science and Practise*, 2nd completely revised and expanded version; Stud. Surf. Sci. and Catal., 137.; Elsevier: Amsterdam, 2001.

(2) Chen, N. Y.; Garwood, W. E.; Dwyer, F. G. *Shape Selective Catalysis in Industrial Applications*; Marcel Dekker: New York, 1989.

(3) Ruthven, D. M. *Principles of Adsorption and Adsorption Processes*; John Wiley and Sons: Canada, 1984.

(4) Brechtelsbauer, C.; Emig, G. *Appl. Catal., A* **1997**, *161*, 79−92.

(5) Brzozowski, R.; Ski, W. *J. Catal.* **2002**, *210*, 313−318.

(6) Bundens, R. G.; Keville, K. M.; Huss, Jr.; Chu, C. T. W.; Husain, A.; Mobil Oil Corporation. Olefin Interconversion by Shape Selective Catalysis. U.S. Patent 5,146,029, 1992.

(7) Calero, S.; Schenk, M.; Smit, B.; Maesen, T. L. M. *J. Catal.* **2004**, *221*, 241−251.

(8) Choudhary, V. R.; Akolekar, D. B. *J. Mol. Catal.* **1990**, *60*, 173−188.

(9) Degnan, J. *J. Catal.* **2003**, *216*, 32−46.

(10) Deniaud, D.; Odobel, F.; Bujoli, B.; Spyroulias, G. A.; Bartoli, J. F.; Battioni, P.; Mansuy, D.; Pinel, C. *New J. Chem.* **1998**, *22*, 901−905.

(11) Ka, J.; Hansildaar, S.; Ponec, V. *J. Catal.* **1997**, *167*, 273−278.

(12) Klemm, E.; Scheidat, H.; Emig, G. *Chem. Eng. Sci.* **1997**, *52*, 2757−2768.

(13) Marcilly, C. R. *Top. Catal.* **2000**, *13*, 357−366.

(14) Llorens, F. J.; Cepeda, E.; Gayubo, A. G.; Aguayo, A. T.; Bilbao, J. *J. Chem. Technol. Biotechnol.* **1998**, *71*, 6−14.

(15) Mostad, H. B.; Riis, T. U.; Ellestad, O. H. *Appl. Catal.* **1990**, *58*, 105−117.

(16) Prasada Rao, T. S. R.; Viswanadham, N.; Murali Dhar, G.; Ray, N. *ACS Symp. Ser.* **1999**, *738*, 130−144.

(17) Villemin, D.; Nechab, B. *React. Kinet. Catal. Lett.* **2000**, *69*, 9−13.

(18) Wang, Y.; Davis, B. H.; Tungate, F. L. *ACS Symp. Ser.* **1999**, *738*, 145−159.

(19) Zhu, W.; Kapteijn, F.; Moulijn, J. A.; Den Exter, M. C.; Jansen, J. C. *Langmuir* **2000**, *16*, 3322−3329.

(20) Cavalcante, J.; Ruthven, D. M. *Ind. Eng. Chem. Res.* **1995**, *34*, 177−184.

(21) Funke, H. H.; Argo, A. M.; Falconer, J. L.; Noble, R. D. *Ind. Eng. Chem. Res.* **1997**, *36*, 137−143.

(22) Huddersman, K.; Klimczyk, M. *AIChE J.* **1996**, *42*, 405−408.

(23) Huddersman, K. *AIChE J.* **1996**, *42*, 2990−2992.

(24) Denayer, J. F.; Souverijns, W.; Jacobs, P. A.; Martens, J. A.; Baron, G. V. *J. Phys. Chem. B* **1998**, *102*, 4588−4597.

(25) Denayer, J. F. M.; Ocakoglu, A. R.; Martens, J. A.; Baron, G. V. *J. Catal.* **2004**, *226*, 240−244.

(26) Denayer, J. F. M.; Ocakoglu, R. A.; De Meyer, K.; Baron, G. V. *Adsorption* **2005**, *11*, 49−53.

(27) Newalkar, B. L.; Kamath, V.; Jasra, R. V.; Bhat, S. G. T. *Adsorption* **1999**, *5*, 345−357.

(28) Newalkar, B. L.; Jasra, R.; Kamath, V.; Bhat, S. G. T. *Microporous Mater.* **1997**, *11*, 195−205.

(29) Santilli, D. S.; Harris, T. V.; Zones, S. I. *Microporous Mater.* **1993**, *1*, 329−341.

(30) Fox, J. P.; Bates, S. P. *J. Phys. Chem. B* **2004**, *108*, 17136−17142.

(31) Lu, L.; Wang, Q.; Liu, Y. *J. Phys. Chem. B* **2005**, *109*, 8845−8851.

(32) Schenk, M.; Calero, S.; Maesen, T. L. M.; Van Benthem, L. L.; Verbeek, M. G.; Smit, B. *Angew. Chem., Int. Ed.* **2002**, *41*, 2499−2502.

(33) Schenk, M.; Calero, S.; Van Benthem, L. L.; Verbeek, M. G.; Schnell, B.; Smit, B.; Maesen, T. L. M.; Vlugt, T. J. H. *J. Catal.* **2003**, *214*, 88−99.

(34) Chempath, S.; Snurr, R. Q.; Denayer, J. F. M.; Baron, G. V. *Stud. Surface Sci. Catal.* **2004**, *154 B*, 1983−1990.

(35) Krishna, R. *Chem. Eng. Res. Des.* **2001**, *79 (2)*, 182−194.

(36) Lawton, S. L.; Leonowicz, M. E.; Partridge, R. D.; Chu, P.; Rubin, M. K. *Microporous Mesoporous Mater.* **1998**, *23*, 109−117.

(37) Meloni, D.; Laforge, S.; Martin, D.; Guisnet, M.; Rombi, E.; Solinas, V. *Appl. Catal., A* **2001**, *215*, 55−66.

(38) Corma, A.; Gonzalezalfaro, V.; Orchilles, A. V. *Appl. Catal., A* **1995**, *129*, 203-215.

(39) Corma, A.; Corell, C.; PerezPariente, J.; Guil, J. M.; GuilLopez, R.; Nicolopoulos, S.; Calbet, J. G.; ValletRegi, M. *Zeolites* **1996**, *16*, 7−14.

(40) Souverijns, W.; Verrelst, W.; Vanbutsele, G.; Martens, J. A.; Jacobs, P. A. *Chem. Commun.* **1994**, 1671−1672.

(41) Dahlhoff, G.; Barsnick, U.; Holderich, W. F. *Appl. Catal., A* **2001**, *210*, 83−95.

(42) Juttu, G. G.; Lobo, R. F. *Microporous Mesoporous Mater.* **2000**, *40*, 9−23.

(43) Kumar, N.; Byggningsbacka, R.; Korpi, M.; Lindfors, L. E.; Salmi, T. *Appl. Catal., A* **2002**, *227*, 97−103.

(44) Park, S. H.; Rhee, H. K. *Appl. Catal., A* **2001**, *219*, 99−105.

(45) Ravishankar, R.; Bhattacharya, D.; Jacob, N. E.; Sivasankar, S. *Microporous Mater.* **1995**, *4*, 83−93.

(46) Denayer, J. F. M.; Ocakoglu, R. A.; Arik, I. C.; Kirschhock, C. E. A.; Martens, J. A.; Baron, G. V. *Angew. Chem., Int. Ed.* **2005**, *44*, 400−403.

(47) Talukdar, A. K.; Bhattacharyya, K. G.; Baba, T.; Ono, Y. *Appl. Catal., A* **2001**, *213*, 239−245.

(48) Wu, P.; Komatsu, T.; Yashima, T. *Microporous Mesoporous Mater.* **1998**, *22*, 343−356.

(49) Zhu, Z. R.; Chen, Q. L.; Zhu, W.; Kong, D. J.; Li, C. *Catal. Today* **2004**, *93*−*95*, 321−325.

(50) Laforge, S.; Martin, D.; Guisnet, M.; Paillaud, J. L. *J. Catal.* **2003**, *220*, 92−103.

(51) Laforge, S.; Martin, D.; Guisnet, M. *Appl. Catal., A* **2004**, *268*, 33−41.

(52) Rigoreau, J.; Laforge, S.; Gnep, N. S.; Guisnet, M. *J. Catal.* **2005**, *236*, 45−54.

(53) Ayrault, P.; Laforge, S.; Martin, D.; Guisnet, M.; Datka, J. *J. Phys. Chem. B* **2004**, *108*, 13755−13763.

(54) Ocakoglu, R. A.; Denayer, J. F. M.; Marin, G. B.; Martens, J. A.; Baron, G. V. *J. Phys. Chem. B* **2003**, *107*, 398−406.

(55) Eder; He, Y. *Recl. Trav. Pays-Bas* **1996**, *115*, 531−535.

(56) Denayer, J. F.; Baron, G. V.; Martens, J. A.; Jacobs, P. A. *J. Phys. Chem. B* **1998**, *102*, 3077−3081.

(57) Ruthven, D. M.; Kaul, B. K. *Adsorption* **1998**, *4*, 269−273.

(58) Zhu, W.; Kapteijn, F.; Van der Linden, B.; Moulijn, J. A. *Phys. Chem. Chem. Phys.* **2001**, *3*, 1755−1761.

(59) Eder, F.; Stockenhuber, M.; Lercher, J. A. *J. Phys. Chem. B* **1997**, *101*, 5414−5419.

(60) Eder, F.; Lercher, J. A. *Zeolites* **1997**, *18*, 75−81.

(61) Atkinson, D. *J. Chem. Edu.* **1978**, *9*, 564−566.

(62) Atkinson, D.; Curthoys, G. *J. Chem. Edu.* **1979**, *56*, 802−804.

(63) Katsanos, N. A. *J. Chem. Soc., Faraday Trans.* **1978**, *74*, 575−582.

(64) Bakaev, V. A. *Adsorption of Hydrocarbons in Microporous Adsorbents − II, Preprints of the Workshop*, Eberswalde/GDR November 22−26, Academy of Sciences of the GDR, Berlin, DDR, **1982**, *1*, 8−17.

(65) Okamura, J. P. *Anal. Chem.* **1971**, *43*, 3 (13), 1730−1733.

(66) Tumsek, F.; Inel, O. *Chem. Eng. J.* **2003**, *94*, 57−66.

(67) Bond. *Appl. Catal., A* **1997**, *160*, 185−190.

(68) Sastre, G.; Catlow, C. R. A.; Chica, A.; Corma, A. *J. Phys. Chem. B* **2000**, *104*, 416−422.

(69) Huang, S. J.; Zhao, Q.; Chen, W. H.; Han, X.; Bao, X.; Lo, P. S.; Lee, H. K.; Liu, S. B. *Catal. Today* **2004**, *97*, 25−34.

(70) Roque-Malherbe, R.; Ivanov, V. *Microporous Mesoporous Mater.* **2001**, *47*, 25−38.

(71) Du, H. W.; Kalyanaraman, M.; Camblor, M. A.; Olson, D. H. *Microporous Mesoporous Mater.* **2000**, *40*, 305−312.

(72) Cejka, J.; Krejci, A.; Zilkova, N.; Kotrla, J.; Ernst, S.; Weber, A. *Microporous Mesoporous Mater.* **2002**, *53*, 121−133.